Metallic nickel nanoparticles supported polyaniline nanotubes as heterogeneous Fenton-like catalyst for the degradation of brilliant green dye in aqueous solution

Madhumita Bhaumik[a*], Arjun Maity[b,c*], Hendrik G. Brink[a*]

[a]*Chemical Engineering Department, University of Pretoria, South Africa.*
[b]*DST/CSIR, Centre for Nanostructure and Advanced Materials (CeNAM), Council for Scientific and Industrial Research (CSIR), Pretoria 0001, South Africa*
[c]*Department of Chemical Science, University of Johannesburg, Doornfontein, 2028 Johannesburg, South Africa.*

Graphical abstract

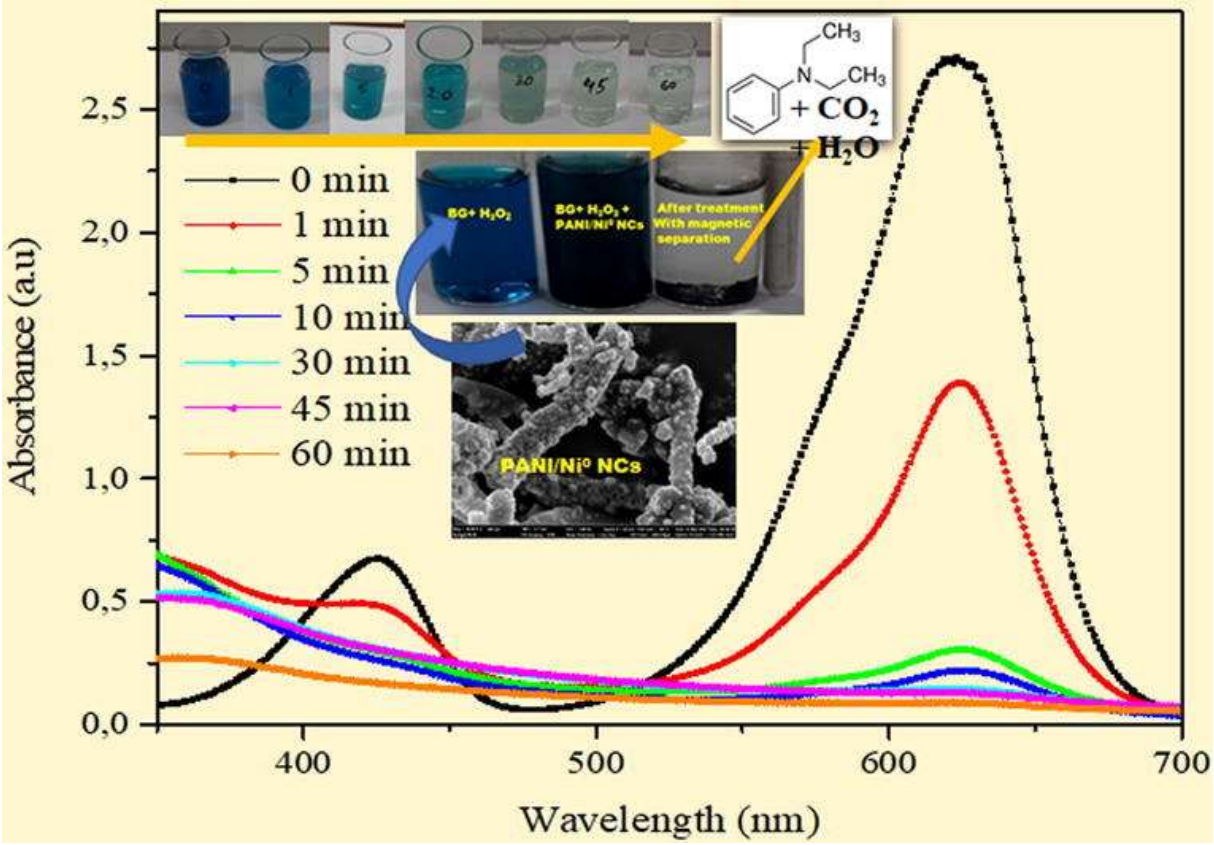

Corresponding authors: bhaumikmadhu@gmail.com (M. Bhaumik); amaity@csir.co.za(A. Maity); deonbrink@up.ac.za(H.G. Brink)

Abstract

Metallic nanoparticles supported on porous matrices are promising heterogeneous catalysts for Fenton-like reaction towards the degradation of organic contaminants in water. Herein, novel magnetic nanocomposites (NCs) of metallic nickel (Ni^0) nanoparticles and nanotubular polyaniline matrix (PANI/Ni^0 NCs) was fabricated by simple reductive formation of Ni^0 nanoparticles upon the pre-synthesized PANI nanotubes (NTs) surface and applied as heterogeneous Fenton-like catalyst in degrading cationic brilliant green dye (BG) in aqueous solution. Various physico-chemical characterization techniques revealed effective supporting of soft ferromagnetic well dispersed nano-dimensional Ni^0 particles onto the PANI NTs matrix. Heterogeneous Fenton-like catalytic performance of PANI/Ni^0 NCs for BG degradation in the presence of hydrogen peroxide (H_2O_2) oxidant demonstrated their superiority when compared with unsupported Ni^0 nanoparticles counterpart. Experiments with a minimum 0.1 g/L of NCs and 10 mM of H_2O_2 displayed complete degradation of 100 mg/L BG within 120 min reaction time. Improved BG degradation was observed with increase in the dose of PANI/Ni^0, H_2O_2 concentration and temperature, whereas it reduced with rise in initial concentration of BG. The rate of degradation was well described by the pseudo-first order kinetic model. Six consecutive BG degradation experiments confirmed NCs reusability without loss of original (~100%) degradation efficiency up to the fifth cycle. Finally, liquid chromatography–mass spectrometric (LC–MS) analyses of the BG samples after 120 min degradation time exposed the formation of N,N-diethyl aniline as degradation product along with partial mineralization of the other end products via the attack of reactive hydroxyl radicals ($HO^{\bullet}$) produced in the catalytic system.

Keywords**:** Polyaniline, Nickel nanoparticles, Nanocomposites, Brilliant green dye, Degradation, Kinetics.

1. Introduction

Synthetic dyes are one of the major contributors for contaminating aquatic environment throughout the world. Among various dyes, brilliant green (BG) is a cationic synthetic dye widely used in textile, paper, paints, plastics, and printing industries and has been reported to be mutagenic and carcinogenic for human health [1]. Moreover, due to high-water solubility industrial effluents containing high levels of BG hinder the photosynthesis cycle of aquatic plants, diminishing oxygen levels in water leading to suffocation of both flora and fauna of the receiving water bodies [2]. Consequently, safe and economic removal of BG dye from wastewater is of prime importance to eliminate its eco toxic hazard effects. A number of treatment techniques including, ion-exchange, adsorption, membrane filtration, flocculation, electro oxidation and ozone/hypochlorite oxidation are effective for decolourization of organic dyes. However, inherent disadvantages associated with high equipment/operation cost, secondary pollution occurring from the spent adsorbent or from residual chlorine have made these methods less attractive for the treatment of dye effluents [3,4]. Conversely, other advanced oxidation processes including photo degradation and Fenton/Fenton-like oxidation have recently been captivated tremendous research interest since these methods involve generation and application of hydroxyl radical ($HO^{\bullet}$) and/or sulfate radicals ($SO_4^{\bullet-}$) in removing/degrading noxious organic pollutants into less toxic species and ultimately to completely mineralized products viz. CO_2, H_2O and/or additional inorganic species [5]. However, it is worth mentioning that the homogeneous Fenton/Fenton-like process which uses metal ions (like Fe^{2+}, Co^{2+}, Mn^{2+} and Ag^{+} etc.) and H_2O_2/persulfates or the UV/H_2O_2/ persulfates system to generate reactive $HO^{\bullet}$ or $SO_4^{\bullet-}$ species for degradation has considerable drawbacks associated with the generation of metal ion containing sludge and the treatment of the produced sludge requires substantial amount of chemicals resulting in extra costs [6]. The innate disadvantages of the homogeneous Fenton or Fenton-like processes could be overcome

using heterogeneous catalyst circumventing secondary pollution and catalyst-recovery step. In fact, various, magnetic nanoparticles have been employed as heterogeneous Fenton-like catalyst for the organic pollutant removal owing to their high catalytic activity, easy phase separation and cost effectiveness [7-9]. However, magnetic nanoparticles (NPs) are susceptible to air oxidation reducing their reactivity and stability. Moreover, nanosized magnetic nanoparticles tend to agglomerate into bigger size particles thereby reducing their reactive surface area. Effective supporting/ immobilization or coating onto porous support matrix have been proven as potential techniques for enhancing the catalytic activity and stability of the magnetic nanoparticles [10-12]. Predominantly magnetic nanoparticles of metallic iron and iron oxides supported on various matrices including clay minerals, porous carbon, carbon nanotubes, carbon nanofibers and graphene oxide have been explored as heterogeneous Fenton-like catalyst for the degradation of organic dyes [13-15]. Although, metallic nickel (Ni^0) nanoparticles due to their high electron donating ability, environmental benignity, unique magnetic properties, and cost effectiveness could efficiently be utilized in catalytic decomposition of organic pollutants, studies regarding the use of Ni^0 based materials as Fenton-like heterogeneous catalysts for the degradation of dyes are limited [11, 16,17]. Generally nanostructured carbon materials have effectively been utilized for support/immobilization of the Ni based magnetic nanoparticles and have been investigated as Fenton-like catalyst towards dye degradation [11,16-17]. However, synthesis of nanocarbon based support matrix commonly uses pyrolysis and complex chemical methods which are cost intensive and produce environmentally hazardous compounds like volatile organics, CO_2, and CO etc. as by-products. Therefore, it is important to explore new cost-effective support matrix for the dispersion/deposition of Ni^0 nanoparticles. Meanwhile, it has already been proved that due to the exceptional electrical properties conductive substrates are superior for nanoparticle catalyst support in comparison with nonconductive one [17]. Consequently, conductive polyaniline

nanotubes (PANI NTs) could serve as a promising reactive support matrix for the immobilization of catalyst nanoparticles owing to the inherent advantages of simple low-cost bulk synthesis method, outstanding suspension ability and environmental benignity [18,19].

In the present study, 2-napthalene sulfonic acid doped PANI NTs synthesized via a self-assembled chemical polymerization technique are employed as support matrix for the facile deposition of Ni^0 nanoparticles through hydrazine reduction of metal precursor. It is anticipated that the as synthesized PANI/Ni^0 nanocomposites (PANI/Ni^0 NCs) would display superior physico-chemical characteristics achieved synergistically from both components of the NCs and could be applied as a heterogeneous Fenton-like catalyst for the degradation of dyes. Superior heterogeneous Fenton-like reactivity for dye degradation possibly be achieved through the catalytic functionality of the as grown Ni^0 nanoparticles in the nanocomposite structures.

Therefore, Fenton-like catalytic performance of the PANI/Ni^0 NCs are investigated for the degradation of BG dye in the presence of hydrogen peroxide (H_2O_2) as oxidant. The effects of various experimental parameters including initial concentration of dye, PANI/Ni^0 NCs dose, H_2O_2 concentration, temperature, radical scavengers on BG degradation are examined in detail. Reaction kinetics and mechanistic pathway of BG degradation are also explored.

2. Materials and experimental methods

2.1. Materials

The reagents including aniline (ANI, 99%,), monomer for PANI polymer, 2-naphthalene sulfonic acid (2-NSA, 70%) used as dopant, ammonium persulfate (APS, 98% purity), the oxidant for polymerization were purchased from Sigma Aldrich, USA. Nickel(II) chloride hexahydrate, precursor for Ni^0 nanoparticles, the reducing agent hydrazine hydrate (50–60%), ethylene glycol (EG), the medium for PANI/Ni^0 synthesis, brilliant green dye (dye

content: 90%), sodium hydroxide, nitric acid, methanol, benzoquinone, t-butanol and all other chemicals used were also acquired from Sigma Aldrich, USA.

2.2. Synthesis of PANI nanotubes

Nanotubular PANI doped with 2-naphthalene sulfonic acid (2-NSA) was synthesized as per the reported synthetic protocols [19]. In a typical synthesis process, ANI (0.2 mL) and the dopant 2-NSA (0.208 g) were mixed with 80 mL ultrapure water with magnetic agitation (200 rpm) for 30 minutes in an ice bath (temperature <5 °C). Afterwards, precooled aqueous solution of APS (0.456 g in 10 mL ultrapure water) was injected into the mixture of 2-NSA and ANI. The mixing condition was continued for additional 1 min to evenly distribute the reaction sites of polymerization. Subsequently, the reaction mixture for polymerization was conserved at 0–5 °C temperature for 24 h without agitation. After completion of polymerization reaction PANI nanotubes were separated from the mixture through vacuum filtration followed by washing with deionized water and acetone. Finally, the as synthesized PANI NTs were dried in a vacuum oven at a temperature of 60 °C for 24 h.

2.3. Synthesis of PANI/Ni^0 nanocomposites

The synthesis of PANI/Ni^0 NCs were performed by supporting Ni^0 nanoparticles onto the PANI NTs matrix. For the preparation of PANI/Ni^0 nanocomposites with ~ 30 wt% Ni^0 nanoparticles loading, $NiCl_2 \cdot 6H_2O$ (0.404 g) was dissolved in 20 mL EG through mechanical agitation. Subsequently, dried powder of PANI NTs (0.2 g) were dispersed into the EG/Ni^{2+} mixture and allowed to attach Ni^{2+} onto the surface of PANI NTs for 3h. Immobilization/supporting of Ni^0 onto the surface of PANI NTs were accomplished by reducing the surface attached Ni^{2+} ions through the addition of hydrazine hydrate (5 mL) and 2 mL of a sodium hydroxide (1 M) solution. For completion of Ni^0 nanoparticles formation,

the reduction reaction was continued for 3h at 60 °C. Afterwards, the as synthesized PANI/Ni^0 NCs were filtered, washed with ultrapure water and ethanol. Finally, the PANI/Ni^0 NCs were dried in a vacuum oven at 60 °C for 24 h. Following the similar synthetic method (barring the use of PANI NTs) bare Ni^0 NPs were also prepared for comparison studies.

2.4. Methods of characterization

A field emission scanning electron microscope (FE-SEM) from Carl Zeiss, Germany, and a high-resolution transmission electron microscope (HR-TEM),) JEM-2100 from JEOL, Japan were employed to investigate the surface morphology and size of the prepared materials, respectively. The Brunauer–Emmett–Teller (BET) surface area of the PANI NTs, Ni^0 nanoparticles and PANI/Ni^0 NCs were determined using the N_2 gas adsorption-desorption apparatus (model ASAP 2420) of Micromeritics, UK. Functional groups of the PANI/Ni^0 NCs were determined by analysing the Fourier transform infrared (FTIR) spectra acquired through a PerkinElmer (USA) attenuated total reflection (ATR) FTIR Spectrum 100 spectrometer. Crystalline structures of the PANI/Ni^0 NCs and PANI NTs were examined by X-ray diffraction patterns obtained with a PANalytical X'Pert PRO diffractometer. Exploration of the elemental compositions and surface oxidation state of Ni^0 NPs within PANI/Ni^0 NCs were confirmed by analysing X-ray photoelectron spectroscopic (XPS) spectrum acquired on an ESCALAB 250Xi XPS spectrometer from Thermo Scientific, USA. Magnetic characterization of the NCs was achieved by a Physical Property Measurements System (PPMS Evercool-II, Quantum Design, USA) in Vibrating Sample Magnetometer (VSM) configuration.

2.5. BG dye removal experiments

Preparation of 1000 mg/L BG dye stock solution was accomplished by the dissolution of 1000 mg of dye into 1L ultrapure water. Dye removal/degradation experiments were

executed in a rotary shaker operated at a speed of 200 rpm. Comparison of dye removal performance of various materials were tested through the addition of 0.025 g of PANI NTs, Ni^0 NPs and PANI/Ni^0 NCs into 250 mL 100 mg/L BG dye solution without pH (solution pH ~ 4.10) adjustment. At regular time intervals, specific volume of aliquots was collected from the reaction vessel and filtered by either centrifugation (for PANI) or magnetically for the analysis of residual dye concentrations. Determination of dye concentration at different time intervals was obtained by noting the UV absorbance value with a UV-1600 PC spectrophotometer at a wavelength of 524 nm. BG dye degradation performance of H_2O_2 oxidant without and with the presence of catalysts was also tested for comparison. Various experimental parameters such as initial BG dye concentration, PANI/Ni^0 dose, H_2O_2 concentration, solution temperature, presence of different scavengers affecting the degradation performance were examined. For the evaluation of recycling ability of the catalyst towards dye removal, 0.5 g/L PANI/Ni^0 was experimented with 20 mg/L BG solution at its original pH (4.21) containing 10 mM of H_2O_2. Followed by first degradation experiment PANI/Ni^0 catalyst was separated from the rection mixture, washed with ultrapure water and ethanol. Finally, it was dried and used for the next cycles of degradation experiment. Six consecutive degradation cycles were tested using the same amount of PANI/Ni^0 NCs. For the assessment of degradation products of BG dye, reaction solution before and after complete colour removal of the dye were subjected to liquid chromatography–quadrupole-time-of-flight mass spectrometry (LC–QTOF-MS) analyses with a Waters UPLC-QTOF MS/MS system. The chromatographic separation was performed on a YMC Hydrosphere C18 reverse phase column followed by a guard column. All the samples were analysed through the electrospray ionization (ESI) method with positive ionization mode.

3. Results and discussion

3.1. Characterization

The FE-SEM image in Fig. 1(a) revealed smooth surfaced nanotubular morphology of 2-NSA doped PANI polymer with an average diameter of 150 nm. In contrary on supporting Ni^0 NPs the surface of PANI becomes coarser associated with an increase in average diameter ~ 210 nm as visualized in Fig. 1(b). Characteristic HR-TEM images of the PANI/Ni^0 NCs as presented in Fig. 2(a) approves successful immobilization of nano-dimensional Ni^0 nanoparticles onto the PANI NTs matrix. Moreover, observed crystal lattice fringes having interplanar spacing ~ 0.203 nm in Fig. 2 (b) suggest (111) crystal planes of the formed Ni^0 nanoparticles [20].

The specific surface areas of the homopolymer PANI, bare Ni^0 nanoparticles and PANI/Ni^0 NCs as calculated via N_2 adsorption-desorption isotherms (Fig. S1) are found to be 29.56, 13.34 and 49.84 m^2/g, respectively. Considerable increase in the specific surface area of the PANI/Ni^0 NCs compared to their constituents would provide larger interfacial area for solid-liquid interaction during degradation process which ostensibly leads to the superior performance of the catalyst. Furthermore, from the pore size distribution data the average pore diameters of 6.7, 5.8 and 6.5 for PANI, Ni^0 and PANI/Ni^0 confirm that all the synthesized materials are mesoporous in nature as their pore diameter are in the typical 2-50 nm range.

The incorporation of emeraldine salt form of 2-NSA doped PANI into PANI/Ni^0 composite nanostructure was confirmed by inspecting the ATR-FTIR spectrum as represented in Fig. 3(a). All the observed vibrational bands with wavenumbers at 1591, 1494, 1281 and 1223, 1163 and 811 cm^{-1} are the characteristic stretching vibrations of C=C bonds in quinoid (Q) and benzenoid (B) rings, C–N bonds inside B and Q-B-Q units, B-NH+ = Q stretching, and C–H bending vibration of aromatic rings within the PANI backbone [21]. The occurrence

of bands at 1037 and 693 cm^{-1} in the FTIR-spectrum of PANI/Ni^0 are typical of sulfonic acid ($-SO_3H^-$) groups attached to the PANI polymer owing to the doping process during polymerization [22].

Representative XRD patterns of the PANI/Ni^0 NCs and PANI homopolymer are displayed in Fig. 3(b). The presence of sharp peaks at 2θ of 44.7°, 52.1° and a minor intensity peak at 76.7° which are associated with X-ray diffraction from (111), (200) and (220) crystal planes of metallic Ni (Ni^0) NPs (JCPDS cards No. 65-0380). Meanwhile, the broad diffraction peaks detected (Fig. 3b) at 2θ of 20.01° and 25.1° resemble the amorphous 2-NSA doped PANI nanostructures [23]. These structural features suggest that crystalline Ni^0 NPs are effectively supported on the amorphous matrix of PANI NTs. The X-ray photoelectron spectroscopic (XPS) survey spectrum representing elemental constituents of PANI/Ni^0 nanocomposites is depicted in Fig. 4(a). The characteristic C 1s, N 1s and S 1s peaks with their respective binding energies appeared in the survey spectrum originated due to the presence of 2-NSA doped PANI polymer, while Ni 2p peak pronounces successful incorporation of Ni species in the composite nanostructures. The high-resolution N 1s spectrum of PANI/Ni^0 as shown in Fig. 4(b) could be deconvoluted into three peaks with corresponding binding energies at 398.9 eV, 399.8 eV and 400.8 eV, respectively. The peak centred at 398.9 eV is the binding energy peak of quinoid imine (=NH-) moieties, whereas the peaks at 399.8 eV and 400.8 eV are typical binding energies of benzenoid amine (-NH-) and positively charged nitrogen ($-N^{\bullet+}$) confirming formation of 2-NSA doped PANI polymer [24]. The core level Ni 2p spectrum in Fig. 4(c) is composed of two main peaks (Ni 2p3/2 and Ni 2p1/2) along with two satellite peaks (sat Ni 2p3/2 and sat Ni 2p1/2) originated from multielectron excitation. The peaks at 855.8 eV and 873.5 eV corresponding to Ni 2p3/2 and Ni 2p1/2 in association with their satellite peaks recommend the occurrence of Ni^{2+} ions species on the surface of PANI/Ni^0 [25]. Additionally, traces of metallic Ni or Ni^0 nanoparticles on the surface of PANI/Ni^0 was detectable owing to

the presence of 2p3/2 binding energy peak centred at 852.5 eV [19]. Ni^0 nanoparticles are highly susceptible to air oxidation which could leads to the formation of surface oxidized Ni^{2+} species of Ni in the form of $Ni(OH)_2$. Magnetic property of PANI/Ni^0 was determined from magnetization vs magnetic field (M-H loop) curve obtained at 300K (room temperature) as displayed in Fig. 4(d). A saturation magnetization (Ms) value of 16.6 emu/g can be perceived from the M-H curve corroborating soft ferromagnetic behaviour of PANI/Ni^0. This weak ferromagnetic behaviour would facilitate ease separation of PANI/Ni^0 from solution after catalytic dye degradation reaction by the application of a simple magnetic field as shown in the inset of Fig. 4(d).

3.2. Catalytic activity assessment of various nanomaterials

Evaluation of the Fenton-like catalytic activity of PANI/Ni^0 NCs along with bare Ni^0 nanoparticles and PANI NTs in presence as well as in absence of H_2O_2 oxidant was performed with BG dye as a model organic pollutant. In order to assess the BG dye degradation ability of H_2O_2 a blank test was also conducted without the use of any catalyst. It can be observed from Fig. 5(a) that degradation of BG in presence of H_2O_2 is insignificant which might be due to the low oxidizing power of H_2O_2 [3]. In the absence of H_2O_2 both PANI/Ni^0 NCs and PANI NTs have shown considerable dye removal efficiencies attributable to their high adsorption affinity towards BG dye. It is worth mentioning that within the very short period of contact time (1 min) almost 76% dye removal was achieved while using PANI/Ni^0 NCs alone. This can be attributed to the high adsorption affinity of PANI/Ni^0 NCs towards BG dye which is the most crucial aspect of using it as heterogeneous catalyst for dye degradation as rapid adsorption can enrich reactant concentration in the proximity of the reaction sites and thereby enhancing the degradation performance. Additionally, it can also be pronounced from Fig. 5(a) that almost 100% decolorization of BG was obtainable with PANI/Ni^0 catalyst in presence of H_2O_2 oxidant

in 120 minutes. These results suggest that PANI/Ni^0 in presence of H_2O_2 performs as a Fenton-like catalyst for the degradation of BG dye. The UV-vis spectra of BG were recorded and depicted in Fig. 5(b) for the elucidation of change in structural features of the dye during degradation reaction. It can be perceived that the absorbance value of the main peak at 624 nm gradually diminishes with the increase in treatment time suggesting adsorption along with degradation of the chromophore groups of the BG dye by PANI/Ni^0 and H_2O_2 oxidant system. At the same time the reduction in absorbance value at 425 nm might be an indication of degradation of the aromatic fragments in the BG cations and its intermediate products. The photograph in the inset of Fig. 5(b) visualizing change in colour of the BG dye with increase in reaction time is consistent with an obvious decrease in absorbance value of the absorption spectra. Meanwhile, a substantial amount of TOC removal as shown in Fig. 5(c) was detected during the BG degradation in the PANI/Ni^0 and H_2O_2 oxidant system, revealing around 90.2% mineralization degrees at 120 min of reaction time. It can be seen from Fig. 5(a) and Fig. 5(c) that although almost 100 % decolorization of BG dye is accomplished within 120 min of reaction time, total mineralization (i.e., 100 %TOC removal) of the intermediates (produced during the degradation process) are not achieved within the similar time interval.

Furthermore, the leached Ni^{2+} ions concentration (560 ppb µg/L) in the reaction solution as analysed by an atomic absorption spectrometer (Perkin Elmer, AAS 100) was considerably below the maximum allowable limit (700 µg/L) implying that the PANI/N^0 NCs primarily act as a heterogeneous Fenton-like catalyst by promoting the release of reactive $HO^{\bullet}$ radicals as represented by the following Eqs.

$$Ni^0 + 2H_2O \rightarrow Ni^{2+} + H_2 + 2OH^- \quad (1)$$

$$H_2O_2 + Ni^{2+} \rightarrow HO^{\bullet} + OH^- + Ni^{3+} \quad (2)$$

$$HO^{\bullet} + BG \rightarrow \text{Degradation products} \quad (3)$$

3.3. Effect of catalyst dose

The effect of PANI/Ni^0 catalyst dose on BG dye degradation efficiency was conducted at an initial concentration of 100 mg/L using three different dose and the obtained results are exhibited in Fig. 6(a). It is noticeable from the figure that dye degradation efficiency increases with an increase in catalyst dose. Specifically, the BG removal efficiencies of 91.72%, 98.00%, and 98.43% were achieved at 120 min degradation time by using 0.1, 0.15, and 0.2 g/L, PANI/Ni^0 catalyst. This could be attributed to facts that increased amount of catalyst provides more active sites for dye adsorption as well as for the decomposition of H_2O_2, which leads to higher BG dye removal performance of PANI/Ni^0 NCs. Meanwhile, the time to reach equilibrium decolorization of BG dye using lower dose of PANI/Ni^0 remains more compared to the higher amount of dose for a specific initial concentration. This feature might be associated with the reduction in total reactive surface area along with active reaction sites accessible to the BG dye molecule due to intermolecular competition and coverage of nickel oxide species onto the Ni^0 nanoparticles surface of the composite nanostructure [26].

3.4. Effect of H_2O_2 concentration

The effect of H_2O_2 concentration (in the range of 1-15 mM) on 100 mg/L BG dye degradation is presented in Fig. 6(b). Improved dye removal efficiency was observed with increase in H_2O_2 concentration. In particular, BG degradation efficiency increased from 83.62% to 99.12% as the H_2O_2 concentration varied from 1 to 10 mM. Enhanced reaction performance at higher concentration of H_2O_2 was obtained through the production of higher number of reactive hydroxyl radicals ($HO^{\bullet}$) involve in dye degradation. Nevertheless, further increase in H_2O_2 concentration to 15 mM is not considerably improved the BG removal efficiency. Slight reduction in dye degradation performance at 15 mM of H_2O_2 usage

experienced from the excessive peroxide loading which induces favourable hydroxyl radicals scavenging effect as follows [27].

$$H_2O_2 + HO^{\bullet} \rightarrow H_2O + HO_2^{\bullet} \quad (4)$$

The $HO_2^{\bullet}$ radicals (have lower oxidation potential than $HO^{\bullet}$) generated from the above type of reaction diminishes the attacking probability of $HO^{\bullet}$ towards oxidation of dye molecules which occasionally reduces degradation performance. Considering optimal degradation performance 10 mM of H_2O_2 was utilized for all subsequent degradation reactions.

3.5. Effect of initial concentration of BG

Initial concentrations of BG solution have significant influence on degradation performance of PANI/Ni^0 NCs as seen in Fig.7(a). It is detected that BG degradation efficiency decreases with increase in initial concentration of dye. A maximum of 99.0% BG dye removal efficiency was achieved at an initial 200 mg/L concentration, whereas the removal efficiency reduced to 91.9% for the concentration of 300 mg/L within 120 min reaction period. The entire removal process of BG could be considered as a two-step heterogeneous reaction which include initial dye adsorption onto PANI/Ni^0 surface followed by oxidative degradation through the combination of PANI/Ni^0 and H_2O_2. Moreover, for a specific amount of PANI/Ni^0 the uptake of BG is fixed. Therefore, increased BG concentration in bulk solution would govern competitive adsorption of BG which subsequently reduces the local concentration of dye molecules in the vicinity of reaction sites and thus leading to lower removal efficiency.

3.6. Kinetic mechanism of BG removal

For the exploration of kinetic mechanism involved in the current degradation reaction the most frequently used pseudo-first-order kinetic model as stated by the Eq. 5 was employed to fit the experimental kinetic data.

$$\frac{C_t}{C_0} = \exp(-k_1 t) \quad (5)$$

where, k_1 (1/min) stands for rate constant of first-order-kinetic model. The nonlinear fitting of kinetic data with pseudo-first-order kinetic model for three different initial concentrations of BG dye is demonstrated in Fig. 7(b). Excellent correlation between experimental kinetic data and pseudo-first-order kinetic model is perceived with corresponding values of correlation coefficients (R^2) as 0.995, 0.995 and 0.977 for 200 mg/L, 250 mg/L and 300 mg/L initial concentrations of BG. The obtained higher values of R^2 signify that kinetic mechanism of BG dye degradation using PANI/Ni^0 catalyst is governed by pseudo-first order kinetic behaviour. This kinetic mechanism for dye degradation using Fenton-like catalyst is in good agreement with the already reported data in the literature [3]. Furthermore, the rate constants (k_1) of pseudo-first-order kinetic model were computed as 0.113/min, 0.048/min, and 0.039/min for the respective 200 mg/L, 250 mg/L and 300 mg/L initial concentration of BG. This result suggests a reduction in rate constant of degradation with increased initial BG dye concentration.

3.7. Effect of reaction temperature

The temperature effect on BG dye degradation efficiency of PANI/Ni^0 was studied at 25 °C, 45 °C and 65 °C and the results are shown in Fig. 8(a). It can be noticed that almost 100 % BG degradation performance was accomplished in 60 min, 30 min and 15 min reaction time for the respective 25 °C, 45 °C and 65 °C temperature. Faster rate of degradation at an elevated temperature might be attributed to rapid transport of dye molecules towards the reaction sites and acquisition of sufficient energy to overcome the activation energy barrier and thereby promoting generation of reactive species for oxidative degradation of BG dye molecule [11]. Additionally, to determine the activation energy of the current catalytic degradation reaction

kinetic rate data obtained at various temperature can be represented in accordance with the Arrhenius equation as expressed in Eq.6.

$$\ln k = \ln A - E_a[\frac{1}{RT}] \quad (6)$$

where k is the pseudo-first order kinetic rate (mg/L/min), A is denoted by frequency factor (mg/L/min), E_a specifies activation energy (kJ/mol), R and T are the respective gas constant (0.008314 kJ/mol/K) and temperature in the absolute scale (K). The ln k versus $1/T$ curve in Fig. 8(b) was employed to calculate activation energy (E_a) and found to be 22.85 kJ/mol for the Fenton-like BG degradation reaction using PANI/Ni^0 in the 25-65 °C temperature range. Higher values of activation energy were reported in the literature for Fe nanoparticles supported materials used for the degradation of dyes in the similar temperature range [3, 28]. The lower value of activation energy obtained in the present degradation system confirms with the fact that Fenton-like oxidative reaction progressed with a low energy barrier [29].

3.8. Effect of scavengers

To confirm the fact that $HO^{\bullet}$ radicals produced due to the PANI/Ni^0 catalyst mediated decomposition of H_2O_2 are the reactive oxygen species involved in the degradation of BG dye several radical scavengers including methanol (MeOH), tert-butanol (t-BuOH) and benzo quinone (BQ) were tested. It can be seen from Fig. 9(a) that ~ 98.2% BG dye was removed in the absence of any radical scavengers. In contrary in presence of t-BuOH and BQ the degradation efficiency of BG was diminished to ~ 60.5% and 35.5%, respectively. Obvious decreases in dye removal performance due to the addition of t-BuOH and BQ is related to their high quenching ability towards $HO^{\bullet}$ radicals presented in the bulk solution as well as bounded on the surface of the catalyst [30]. However, negligible radical scavenging effect was observed for MeOH on degradation of BG using PANI/Ni^0. This is indicative of the fact that

hydrophilicity of MeOH inhibits it to reach the catalyst surface and thereby restricts to capture the surface adsorbed $HO^{\bullet}$ radicals entirely [31]. These findings suggest the participation of HO• radicals (generated in the Fenton-like PANI/Ni^0+H_2O_2 system) for the degradation of BG dye which are in conformity with recently reported results in the literature [32,33].

3.9. Recyclability of PANI/Ni^0 NCs

Recyclability or reusability of the PANI/Ni^0 NCs is a prime aspect in assessing its cost effectiveness as a catalyst media for dye degradation. With this perspective, consecutive BG dye degradation experiments were performed using the same sample media (PANI/Ni^0 NCs) under similar reaction conditions. Followed by each cycle of BG degradation experiments, PANI/Ni^0 NCs were separated from reaction medium by filtration, washed with ultrapure water and ethanol. The spent PANI/Ni^0 NCs were used for the successive cycle of BG removal. The BG dye removal performance of the PANI/Ni^0 NCs experiencing six degradation cycles is demonstrated in Fig. 9(b). It can be perceived that up to 5^{th} cycle almost 100% BG removal efficiency was achievable within 120 min of degradation reaction. However, in the 6^{th} cycle degradation efficiency decreased to 94.5%, suggesting trivial loss of catalytic activity of the PANI/Ni^0 NCs. Reduction in BG removal performance can be attributed to the probable formation of $Ni(OH)_2$ or NiO in the presence of OH^- ions and dissolved oxygen. These oxide/hydroxide species of Ni can easily be leached to the solution leaving inner core of Ni^0 for subsequent reaction and thus reducing catalytic activity of the PANI/Ni^0 NCs in the 6^{th} cycle. Therefore, PANI/Ni^0 NCs can be effectively used as catalyst media up to five consecutive cycles without sacrificing its original (~100%) degradation efficiency towards BG dye.

3.10. Degradation products identification and exploration of degradation pathways

QTOF-LC-MS/MS analyses were conducted in order to identify the degradation products of BG dye in Fenton-like reaction using PANI/Ni^0 catalyst as well as to explore the possible pathways of degradation. Figure 10 displays the obtained chromatograms (along with the mass to-charge ratio(m/z) of obtained different molecular species) of the BG solution (50 mg/L) before and after treatment with PANI/Ni^0 (0.1 g/L) and 10 mM of H_2O_2. The chromatogram of blank sample is also presented in Fig. 10A(a) for comparison. Fig. 10A(b) shows the chromatogram of BG dye before degradation reaction. A comparison of Fig. 10A(a) and 10A(b) revealed that the peak appeared with the m/z value of 385.26 corresponds to the cationic BG dye. It can be observed from Fig. 10B(c) that the obtained chromatogram of BG after degradation reaction time of 30 min is almost identical with chromatogram of BG (Fig. 10A(b)) acquired before degradation apart from the appearance of two new peaks with m/z values of 357.23 and 254.15, respectively. Increasing the treatment time from 30 min to 120 min directed to the formation of degradation end product N,N-diethyl aniline with characteristic m/z value of 149.02 as demonstrated in Fig. 10B(d). The appearance of new peaks is due to the degradation of BG by Fenton-like reaction using H_2O_2 and PANI/Ni^0 NCs catalyst. It is worth noticing in Fig. 10B(d) that the abundance of N,N-diethyl aniline (m/z value149.02) in the reaction solution become trivial suggesting low molecular weight degradation products might reduce to carbon dioxide and water including other inorganics. The BG dye degradation products found at m/z ratios of 357.23, 254.15 and 149.02 are consistent with the results reported by Rao et al and Rehman et al. [34,35].

The active participation of reactive oxygen species, $HO^{\bullet}$ produced in the present Fenton-like reaction system could be utilized in order to explore the formation pathways of the detected degradation products of the BG dye. The degradation products formation routes are presented in the Scheme 1. The degradation product with m/z value 357.23 originated due to

the de-ethylation at the side ethyl group of BG by reactive $HO^{\bullet}$ radicals as it has been well documented that $HO^{\bullet}$ could play an important role in the elimination of ethyl groups from organic compounds [35]. The removal of H atom from ethyl group resulted to the production of carbon centred radical which can lead to the formation of peroxy radical in presence of oxygen. The exclusion of $HO_2^{\cdot}$ group from peroxy radical followed by the reaction with H_2O originating the degradation product with m/z value 357.23. Meanwhile, the cleavage of bond between position 1 and 2 by $HO^{\bullet}$ followed by hydroxylation mechanism governs to the appearance of the degradation product with m/z 254.18. The formation of the final degradation product i.e., N,N diethyl aniline with m/z value of 149.02 can be attributed to fact of electrophilic attack by $HO^{\bullet}$ at the more nucleophilic central carbon atom of BG [36]. Therefore, the LC-MS/MS analyses results suggest that the mechanism towards the production of degradation products of BG in the current Fenton- like system using H_2O_2 and PANI/Ni^0 catalyst primarily proceeds through the direct involvement of the generated reactive $HO^{\bullet}$ radicals.

4. Conclusions

In this study, nanocomposites of PANI/N^0 were synthesized by the reductive deposition of Ni^0 nanoparticles on the 2-NSA doped PANI NTs surface. The as prepared magnetic PANI/N^0 NCs possessed improved surface area compared to their constituents enabling superior performance towards solid-liquid interfacial reactions. Application of PANI/Ni^0 NCs as heterogeneous Fenton-like catalyst for the degradation BG dye in aqueous solution with H_2O_2 oxidant showed enhanced degradation performance compared to the bare Ni^0 nanoparticles. Effective supporting of Ni^0 nanoparticles onto the reactive PANI NTs matrix having strong adsorption affinity towards BG increases the local concentration of the dye at the catalytic sites of the NCs thereby attributing to higher degradation performance. The

degradation efficiency of PANI/Ni^0 was noticeably influenced by the doses of catalyst, initial concentration of BG, H_2O_2 concentration and temperature. The kinetic mechanism of BG degradation was well correlated with the pseudo-first order kinetic model. Significantly lower activation energy (22.85 kJ/mol) was required for the present degradation reaction. Among various radical scavengers' presence of benzo quinone (BQ) largely affected the BG degradation efficiency of PANI/Ni^0 NCs. Identification of BG dye degradation products using LC–MS/MS method explored that N,N diethyl aniline was the end product yielded after 120 min of reaction in association with possible fractional mineralization in the form of CO_2 and H_2O. Meanwhile, six consecutive recycling experiments established that the PANI/Ni^0 NCs could be reused up to fifth degradation cycle without loss of original (~100%) catalytic efficiency. Therefore, excellent degradation performance, good recycling ability and easy magnetic separation from reaction vessel supports the potential feasibility of PANI/Ni^0 catalyst for the treatment of industrial wastewater containing recalcitrant organic pollutants.

Acknowledgement

MB is appreciative to the University of Pretoria, South Africa, for providing a post-doctoral fellowship and National Research Foundation (NRF) for financial support. The authors like to acknowledge the chemical engineering department, University of Pretoria, South Africa, for providing infrastructure for the research activity. The authors would also like to thank Prof. VV Srinivasu, University of South Africa, South Africa, for characterizing the magnetic property of the material using PPMS system.

References

[1] V.L. Gole, P.R. Gogate, Degradation of brilliant green dye using combined treatment strategies based on different irradiations, Sep. Purif. Technol. 133 (2014) 212–220.
[2] M. Iram, C. Guo, Y. Guan, A. Ishfaq, H. Liu, Adsorption and magnetic removal of neutral red dye from aqueous solution using Fe_3O_4 hollow nanospheres, J. Hazard. Mater. 181 (2010) 1039–1050.
[3] J.H. Ramirez, F.J. Maldonado-Ho´dar, A.F. Pe´rez-Cadenas, C. Moreno-Castilla, C.A. Costa, L.M. Madeira, Azo-dye Orange II degradation by heterogeneous Fenton-like reaction using carbon-Fe catalysts, Applied Catalysis B: Environmental 75 (2007) 312–323.
[4] M. Panizza, G. Cerisola, Direct and mediated anodic oxidation of organic pollutants, Chem. Rev. 109 (2009) 6541−6569.
[5] M. Trojanowicz, A. Bojanowska-Czajka, I. Bartosiewicz, K. Kulisa, Advanced oxidation/reduction processes treatment for aqueous perfluorooctanoate (PFOA) and perfluorooctanesulfonate (PFOS) – a review of recent advances, Chem. Eng. J. 336 (2018) 170–199.
[6] T. Zeng, X. Zhang, S. Wang, H. Niu, Y. Cai, Spatial confinement of a Co_3O_4 catalyst in hollow metal—organic frameworks as a nanoreactor for improved degradation of organic pollutants, Environ. Sci. Technol. 49 (2015) 2350–2357.
[7] Z. Fang, X. Qiu, J. Chen, X. Qiu, Degradation of metronidazole by nanoscale zero-valent metal prepared from steel pickling waste liquor, Appl. Catal. B: Environ. 100 (2010) 221–228.
[8] S.Q. Liu, L.R. Feng, N. Xu, Z.G. Chen, X.M. Wang, Magnetic nickel ferrite as a heterogeneous photo-Fenton catalyst for the degradation of rhodamine B in the presence of oxalic acid, Chem. Eng. J. 203 (2012) 432–439.
[9] P. Avetta, A. Pensato, M. Minella, M. Malandrino, V. Maurino, C. Minero, K. Hanna, D. Vione, Activation of persulfate by irradiated magnetite: implications for the degradation of phenol under heterogeneous photo-Fenton-like conditions, Environ. Sci. Technol. 49 (2015) 1043–1050.
[10] F. Duarte, F.J. Maldonado-Hódar, L.M. Madeira, Influence of the particle size of activated carbons on their performance as Fe supports for developing Fenton-like catalysts, Ind. Eng. Chem. Res. 51(2012) 9218–9226.
[11] Y. Yao, H. Chen, C. Lian, F. Wei, D. Zhang, G, Wu, B. Chen, S. Wang, Fe, Co, Ni nanocrystals encapsulated in nitrogen-doped carbon nanotubes as Fenton-like catalysts for organic pollutant removal, J. Hazard. Mater. 314 (2016) 129–139.
[12] L. Yu, J. Chen, Z. Liang, W. Xu, L. Chen, D. Ye, Degradation of phenol using Fe_3O_4-GO nanocomposite as a heterogeneous photo-Fenton catalyst, Sep. Purif. Technol. 171(2016) 80–87.
[13] A. Rodrı´guez, G. Ovejero, J. L. Sotelo, M. Mestanza, J. Garcı´a, Heterogeneous Fenton catalyst supports screening for mono azo dye degradation in contaminated wastewaters, Ind. Eng. Chem. Res. 49 (2010) 498–505.
[14] S. Song, Y. Wang, H. Shen, J. Zhang, H. Mo, J. Xie, N. Zhou, J. Shen, Ultrasmall graphene oxide modified with Fe_3O_4 nanoparticles as a Fenton-like agent for methylene blue degradation, ACS Appl. Nano Mater.11 (2019) 7074–7084.
[15] N. Thomas, D.D. Dionysiou, Suresh C. Pillai, Heterogeneous Fenton catalysts: A review of recent advances, J. Hazard. Mater. 404 (2021) 124082.
[16] J. Kang, X. Duan, C. Wang, H. Sun, X. Tan, M.O. Tade, S. Wang, Nitrogen-doped bamboo-like carbon nanotubes with Ni encapsulation for persulfate activation to remove emerging contaminants with excellent catalytic stability, Chem. Eng. J. 332 (2018) 398–408.
[17] Y. Yao, J. Zhang, M. Gao, M. Yu, Y. Hu, Z. Cheng, S. Wang, Activation of persulfates

by catalytic nickel nanoparticles supported on N-doped carbon nanofibers for degradation of organic pollutants in water, J. Colloid Interf. Sci. 529 (2018) 100–110.
[18] L. Kong, X. Lu, E. Jin, S. Jiang, C. Wang, W. Zhang, Templated synthesis of polyaniline nanotubes with Pd nanoparticles attached onto their inner walls and its catalytic activity on the reduction of p-nitroanilinum, Composites Sci. Technol. 69 (2009) 561–566.
[19] M. Bhaumik, A. Maity, H.G. Brink, Zero valent nickel nanoparticles decorated polyaniline nanotubes for the efficient removal of Pb(II) from aqueous solution: Synthesis, characterization and mechanism investigation, Chem. Eng. J. 417 (2021) 127910.
[20] Z.W. Zhao, X, Zhou, Y.N. Liu, C.C. Shen, C.Z. Yuan, Y.F. Jiang, S.J. Zhao, L.B. Ma, T.Y. Cheang, A.W. Xu, Ultrasmall Ni nanoparticles embedded in Zr-based MOFs provide high selectivity for CO_2 hydrogenation to methane at low temperatures, Catal. Sci. Technol. 8 (2018) 3160-3165.
[21] Z. Zhang, Z. Wei, L. Zhang, M. Wan, Polyaniline nanotubes and their dendrites doped with different naphthalene sulfonic acids, Acta Mater. 53 (2005) 1373–1379.
[22] J. Huang, M. Wan, In situ doping polymerization of polyaniline microtubules in the presence of β-naphthalene sulfonic acid, J. Polym. Sci. A: Polym. Chem. 37 (1999) 151–157.
[23] M. Bhaumik, V.K. Gupta, A. Maity, Synergetic enhancement of Cr(VI) removal from aqueous solutions using polyaniline@$Ni(OH)_2$ nanocomposites adsorbent, J. Environ. Chem. Eng. 6 (2018) 2514–2527.
[24] X.L. Wei, M. Fahlman, A.J. Epstein, XPS study of highly sulfonated polyaniline, Macromolecules 32 (1999) 3114–3117.
[25] L. L. Wang, D. F. Zhang, L. Guo, Phase-segregated Pt–Ni chain-like nanohybrids with high electrocatalytic activity towards methanol oxidation reaction**,** Nanoscale, 6 (2014) 4635–4641.
[26] M. Bhaumik, R.I. McCrindle, A. Maity, Enhanced adsorptive degradation of Congo red in aqueous solutions using polyaniline/Fe^0 composite nanofibers, Chem. Eng. J. 260 (2015) 716–729.
[27] J. De Laat, T.G. Le, Effects of chloride ions on the iron(III)-catalyzed decomposition of hydrogen peroxide and on the efficiency, Appl. Catal. B: Environ. 66 (2006) 137-146.
[28] W. Wang, Y. Cheng,T. Kong, G. Cheng, Iron nanoparticles decoration onto three-dimensional graphene for rapid and efficient degradation of azo dye, J. Hazard. Mater. 299 (2015) 50–58.
[29] S.P. Sun, C.J. Li, J.H. Sun, S.H. Shi, M.H. Fan, Q. Zhou, Decolorization of an azo dye Orange G in aqueous solution by Fenton oxidation process: Effect of system parameters and kinetic study, J. Hazard. Mater. 161 (2009) 1052–1057.
[30] X. Wang, Y. Qin, L. Zhu, H. Tang, Nitrogen-doped reduced graphene oxide as a bifunctional material for removing bisphenols: synergistic effect between adsorption and catalysis, Environ. Sci. Technol. 49 (2015) 6855–6864.
[31] Y. Yao, J. Zhang, M. Gao, M. Yu, Y. Hu, Z. Cheng, S. Wang, Activation of persulfates by catalytic nickel nanoparticles supported on N-doped carbon nanofibers for degradation of organic pollutants in water, J. Colloid Interf. Sci. 529 (2018) 100–110.
[32] J.A. Khan, X. He, H.M. Khan, N.S. Shah, D.D. Dionysiou, Oxidative degradation of atrazine in aqueous solution by UV/H_2O_2/Fe^{2+}, UV/$S_2O_8^{2-}$/Fe^{2+} and UV/HSO_5^-/Fe^{2+} processes: a comparative study, Chem. Eng. J. 218 (2013) 376–383.
[33] F. Chen, S. Xie, X. Huang, X. Qiu, Ionothermal synthesis of Fe_3O_4 magnetic nanoparticles as efficient heterogeneous Fenton-like catalysts for degradation of organic pollutants with H_2O_2, J. Hazard. Mater. 322 (2017) 152–162.
[34] Ch.V. Rao, A.S. Giri, V.V. Goud, A.K. Golder, Studies on pH-dependent color variation and decomposition mechanism of brilliant green dye in Fenton reaction, Int. J. Ind. Chem. 7 (2016) 71–80.

[35] F. Rehman, M. Sayed, J.A. Khan, N.S. Shah, H.M. Khan, D.D. Dionysioua Oxidative removal of brilliant green by UV/$S_2O_8^{2-}$, UV/HSO_5^- and UV/H_2O_2 processes in aqueous media: A comparative study, J. Hazard. Mater. 357 (2018) 506–514.
[36] J.S. Chen, M.C. Liu, J.D. Zhang, Y.Z. Xian, L.T. Jin, Electrochemical degradation of bromopyrogallol red in presence of cobalt ions, Chemosphere 53 (2003) 1131–1136.

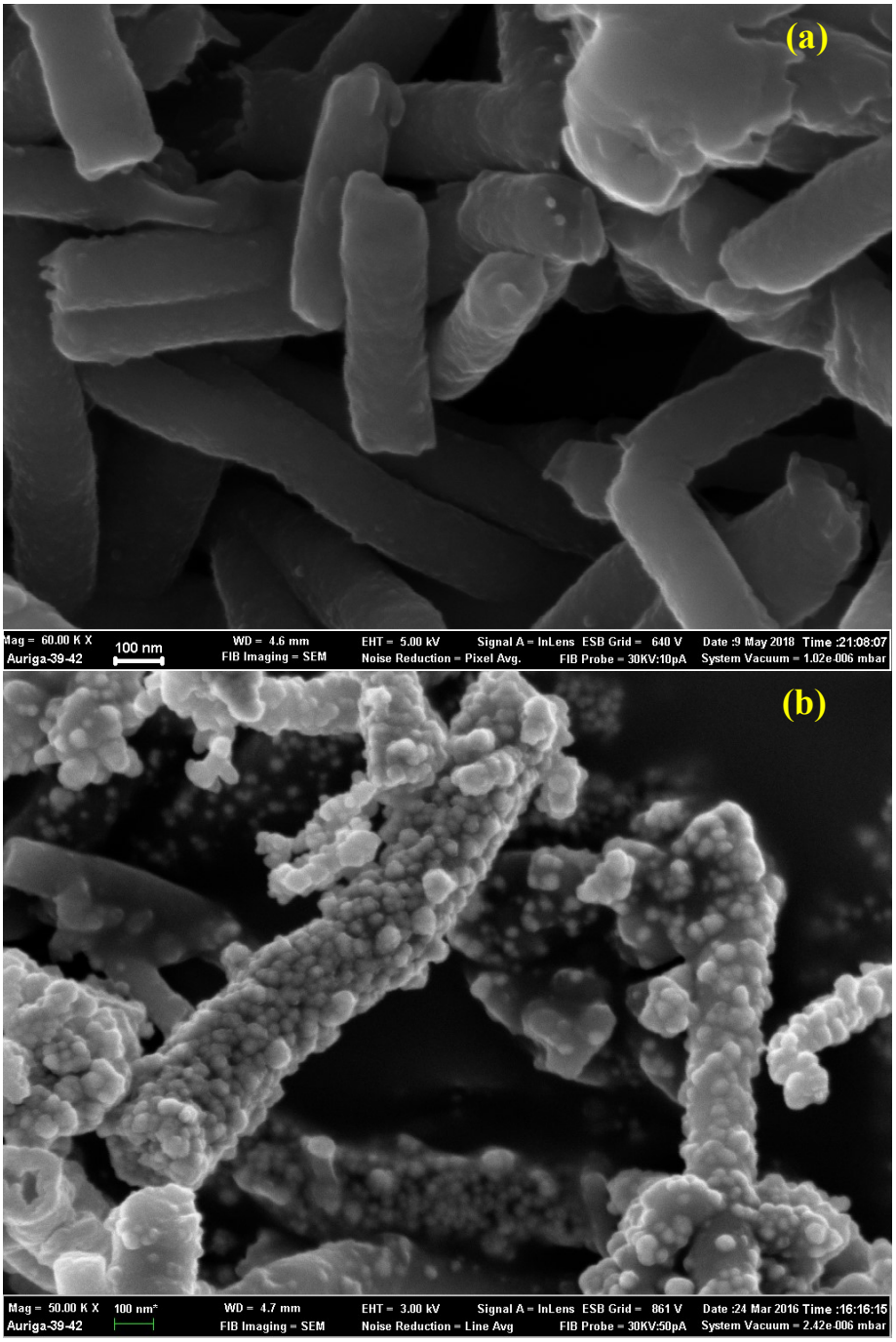

Fig. 1. FE-SEM images of (**a**) PANI NTs and (**b**) PANI/Ni^0 NCs.

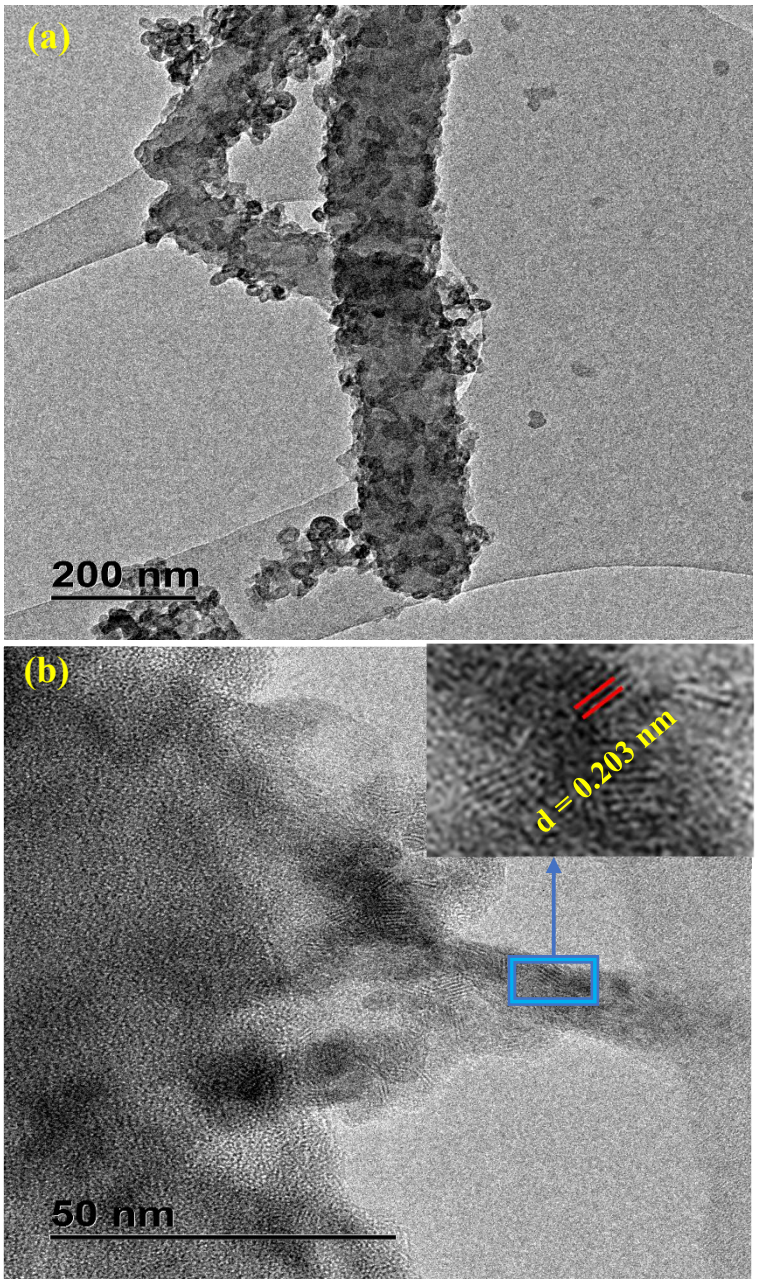

Fig. 2. HR-TEM images of (**a**) and (**b**) PANI/Ni^0 NCs at two different magnifications, inset of (**b**): crystal lattice fringes of Ni^0 nanoparticles within PANI/Ni^0 NCs.

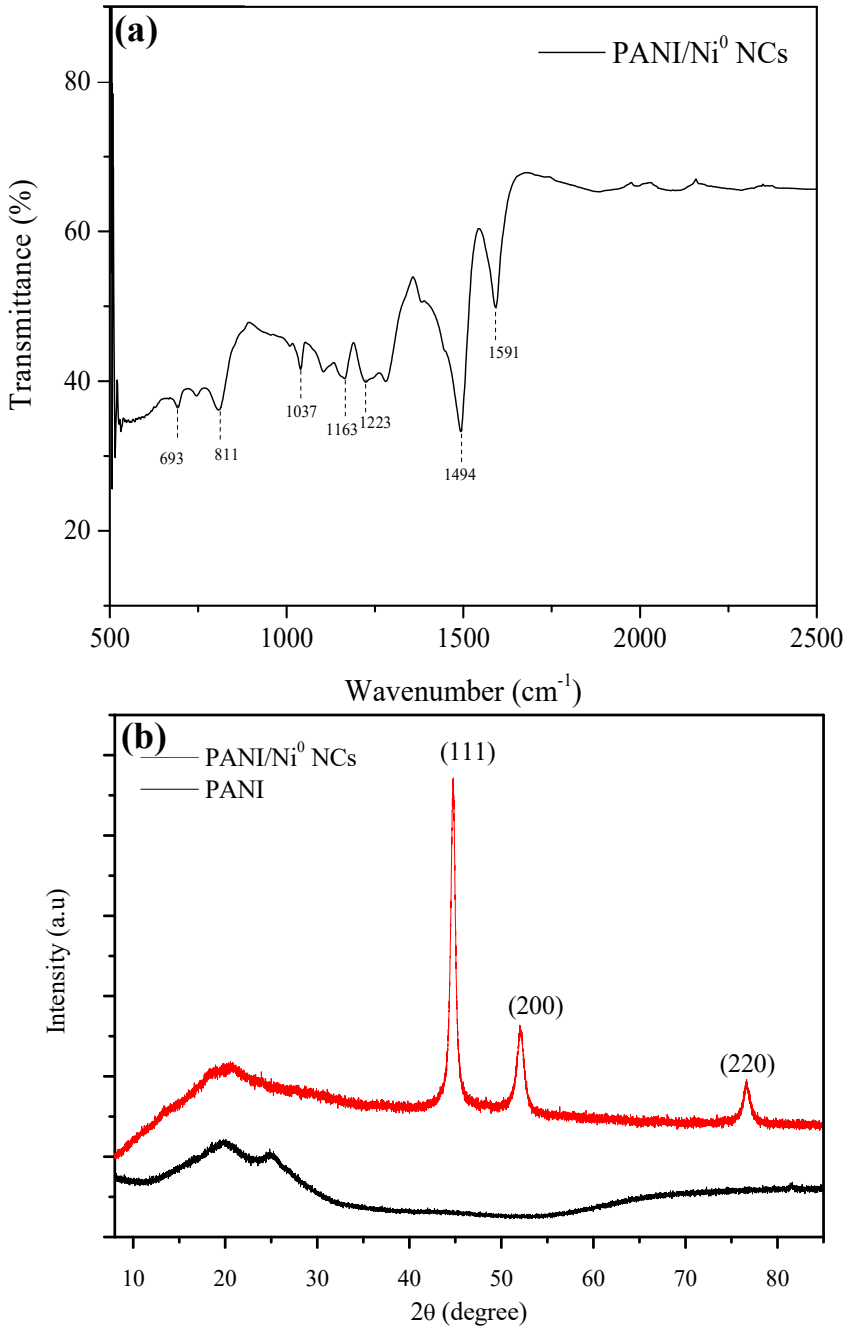

Fig. 3. (a) ATR-FTIR spectrum of PANI/Ni^0 NCs and (b) XRD patterns of PANI/Ni^0 NCs and PANI nanotubes.

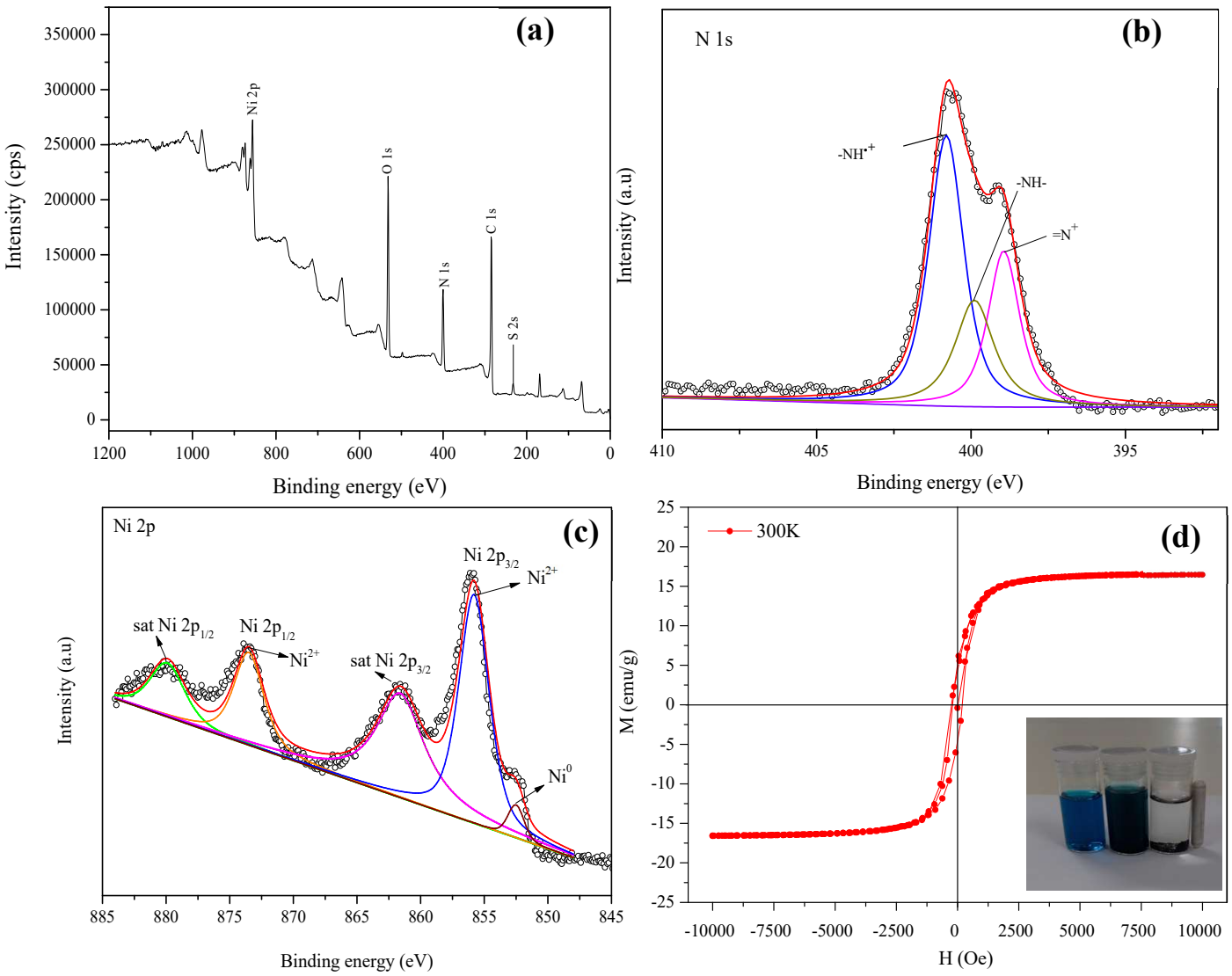

Fig. 4. (a) XPS survey spectrum of the PAN/Ni^0 NCs before BG degradation (b) N1s core level spectrum of PANI/Ni^0 NCs, (c) Ni 2p spectrum of the PANI/Ni^0 NCs before BG removal and (d) Magnetic hysteresis loop of the PANI/Ni^0 NCs at 300K (inset: separation of PANI/Ni^0 NCs after BG treatment).

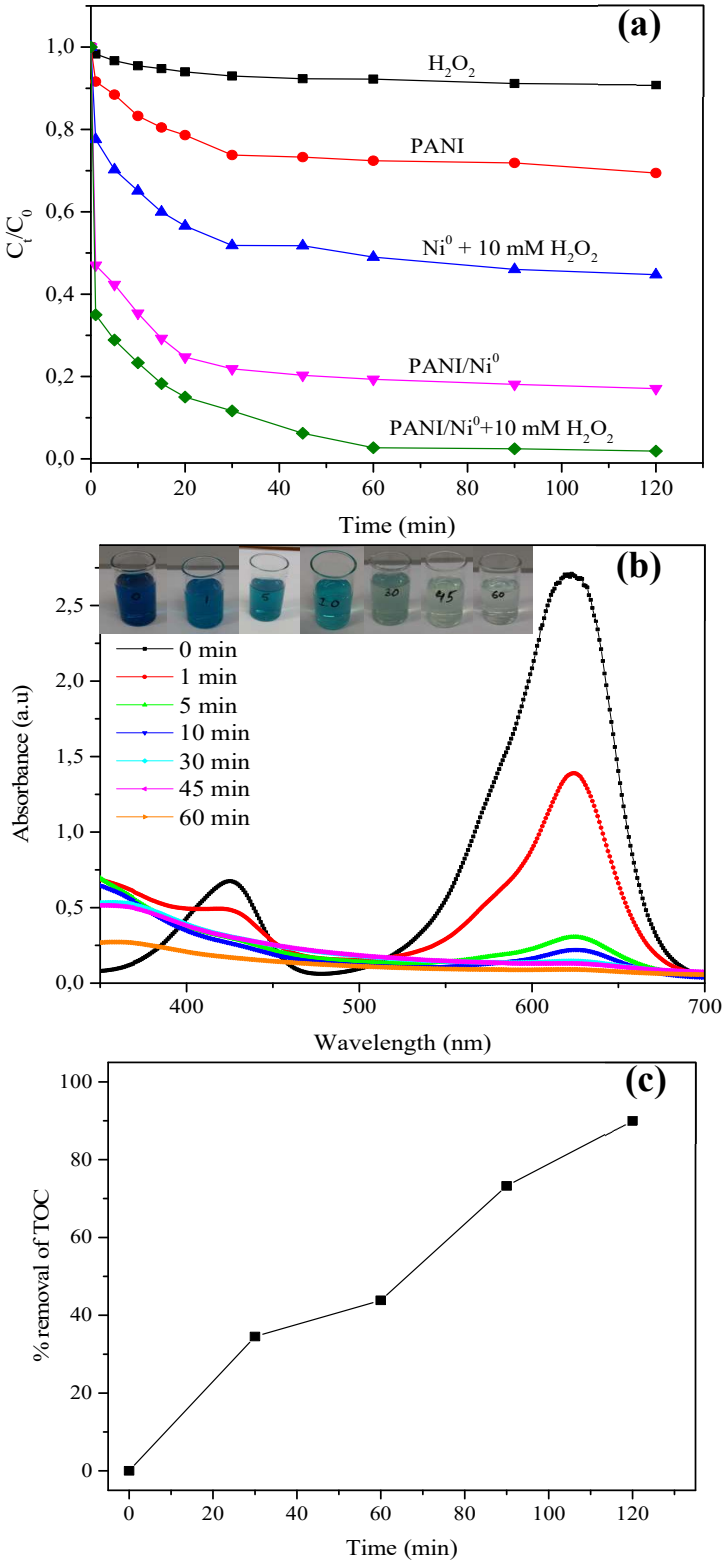

Fig. 5. (a) Comparison of BG degradation efficiencies using various materials, at a dose: 0.1g/L for each set, (b) UV–vis spectra of BG at different treatment time using PANI/Ni^0 + 10 mM H_2O_2 system (inset: photograph of the corresponding colour change at various reaction times) and (c) TOC removal efficiency using PANI/Ni^0 NCs + 10 mM H_2O_2 at selected time intervals.

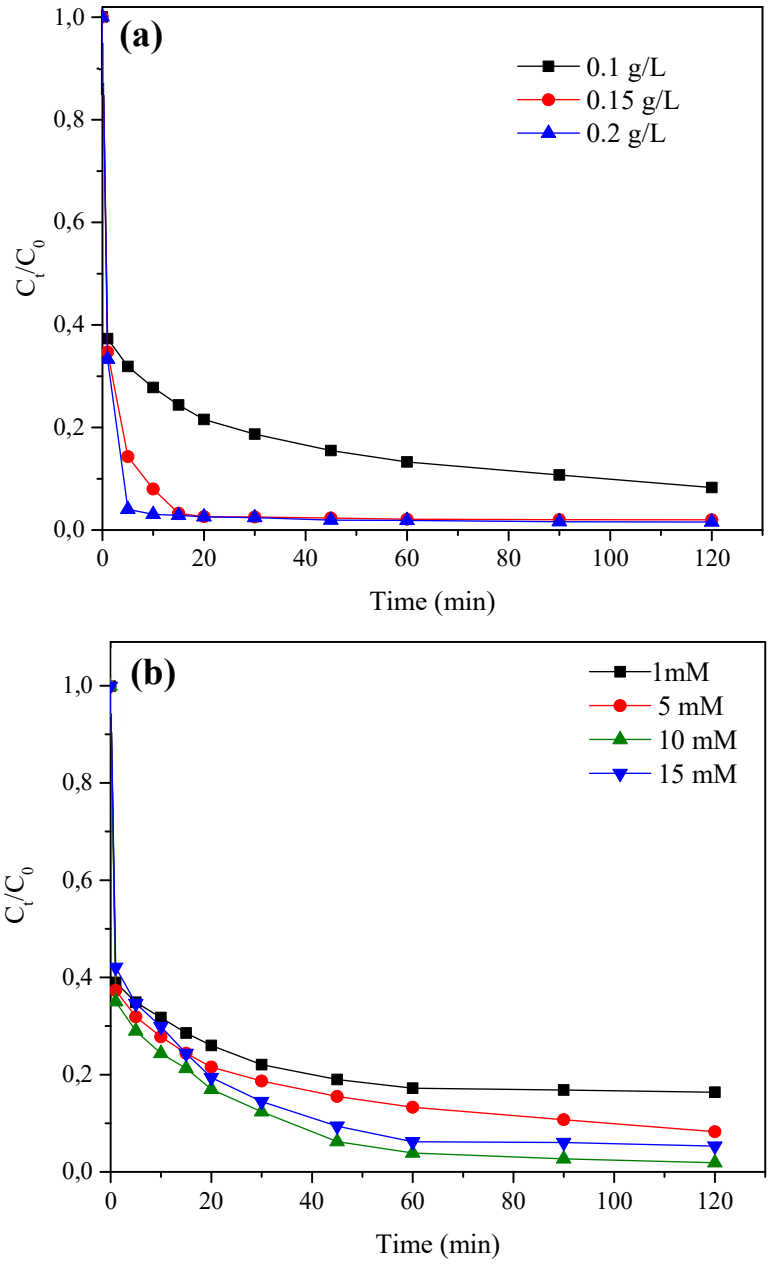

Fig. 6. (a) Effect of PANI/Ni^0 NCs dose on the degradation of BG (initial con.:100 mg/L, H_2O_2 con.: 5 mM) and (b) effect of H_2O_2 oxidant concentration on the removal of BG using PANI/Ni^0 NCs (initial con.:100 mg/L, dose: 0.1 g/L).

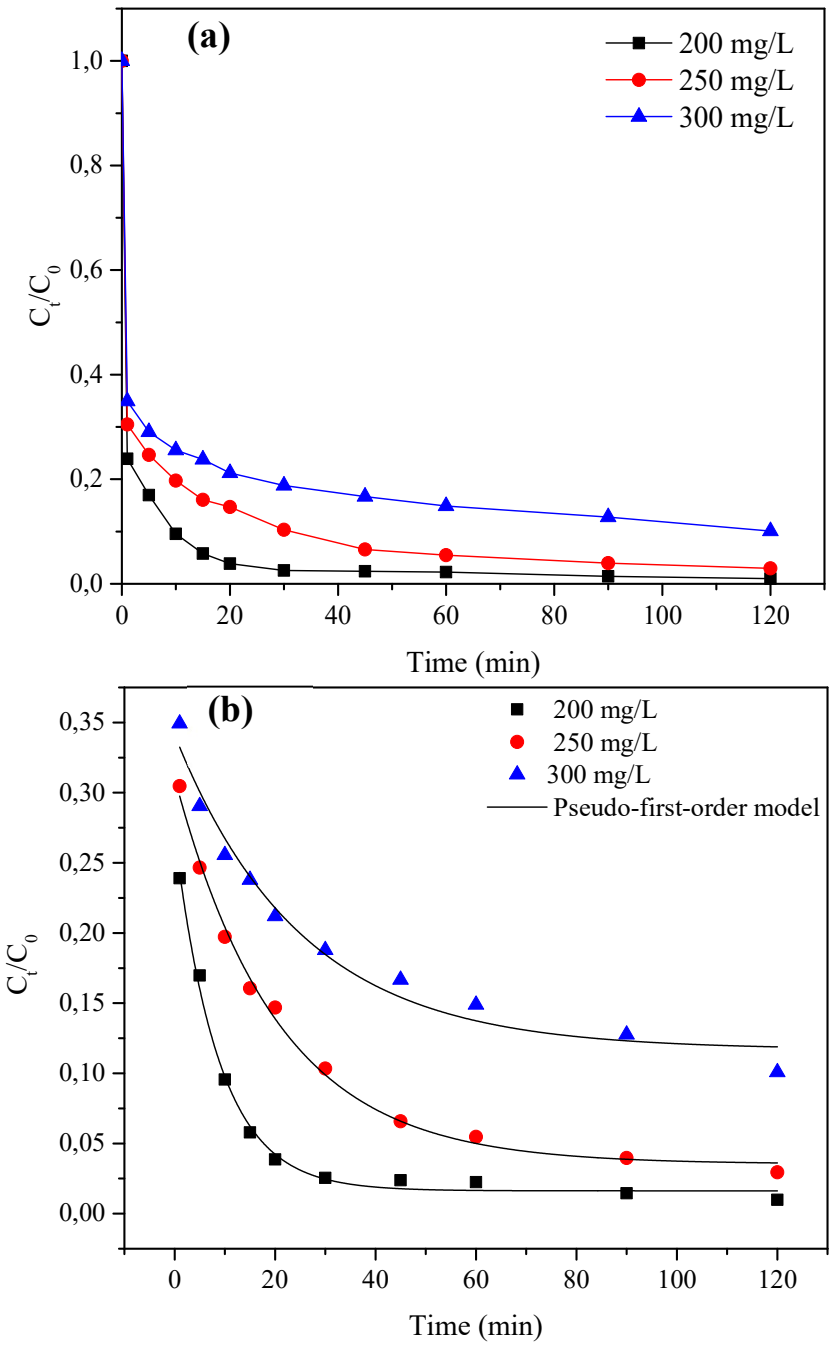

Fig. 7. (a) Effect of initial concentrations of BG degradation using PANI/Ni^0 NCs + 10 mM H_2O_2 (dose: 0.2g/L) and (b) pseudo-first-order kinetic model fitting for removal of BG onto PANI/Ni^0 NCs + 10 mM H_2O_2.

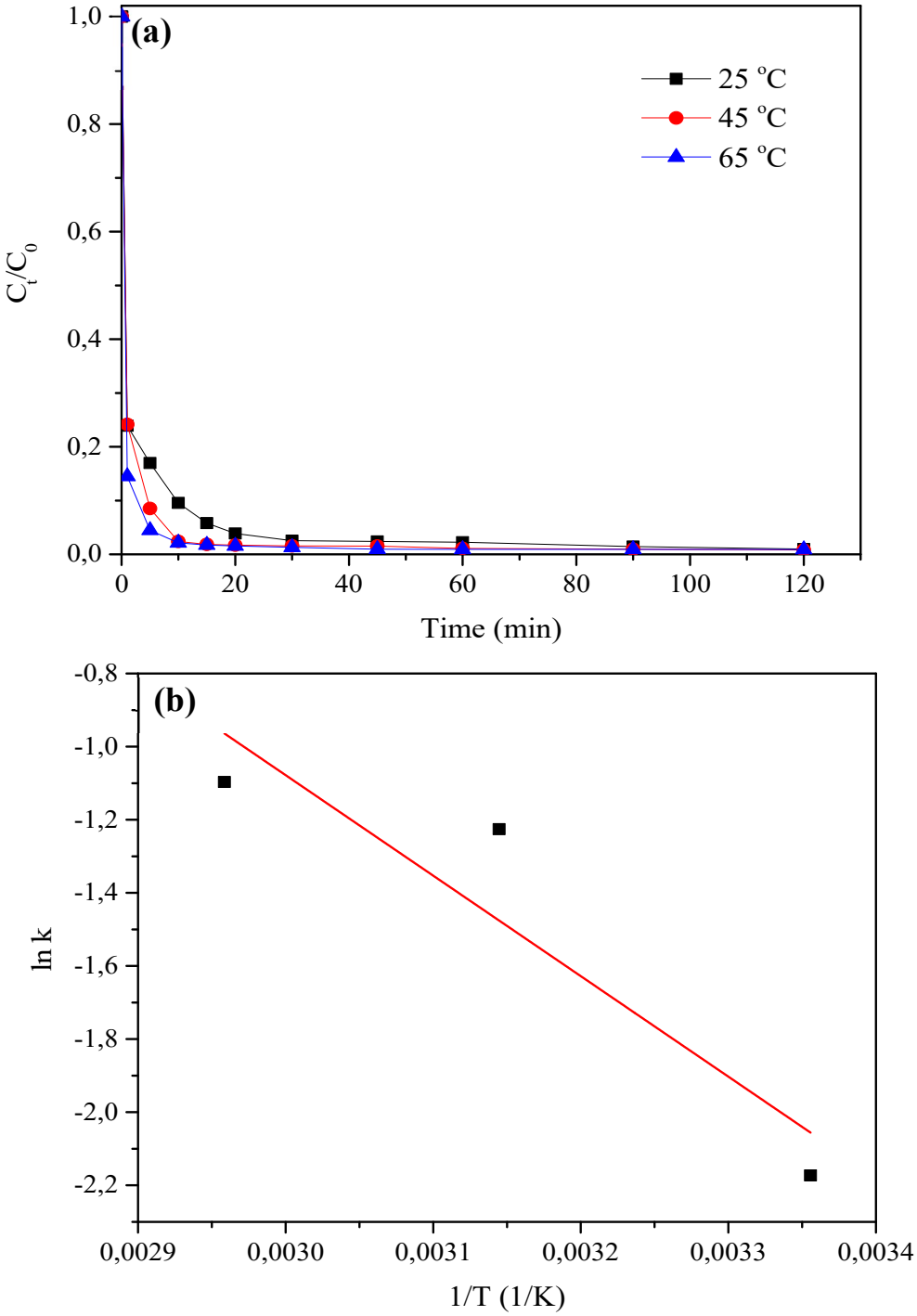

Fig. 8. (a) Effect of temperature on the degradation efficiency of PANI/Ni^0 NCs + 10 mM H_2O_2 and (b) Arrhenius plot of ln*k* versus 1/T for the calculation of activation energy of BG degradation.

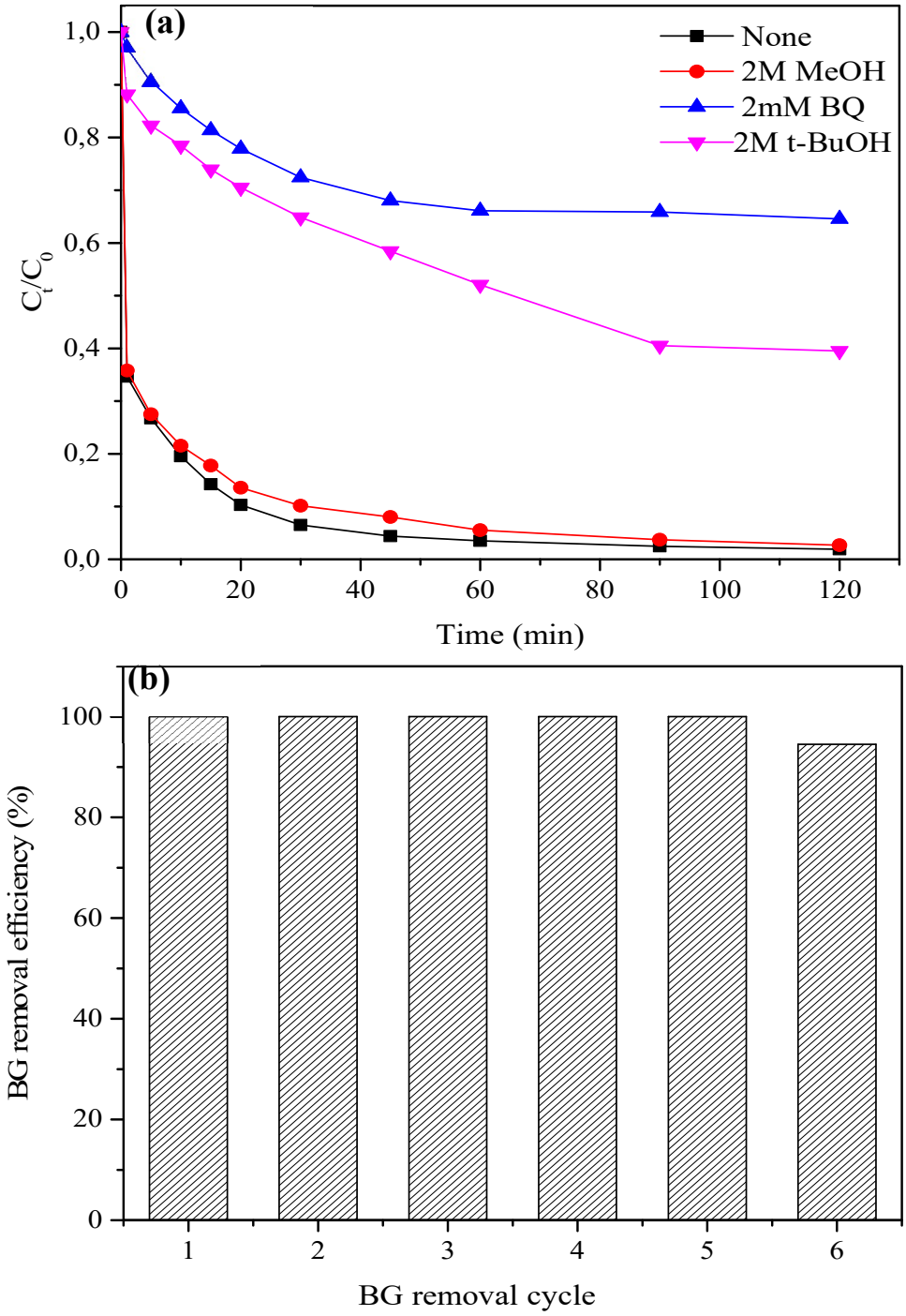

Fig. 9. (a) Effects of scavengers on the BG degradation by the PANI/Ni^0 NCs + 10 mM H_2O_2 system (initial con.: 100 mg/L, dose: 0.1 g/L) and (b) Recycling efficiency of PANI/Ni^0 NCs towards BG degradation.

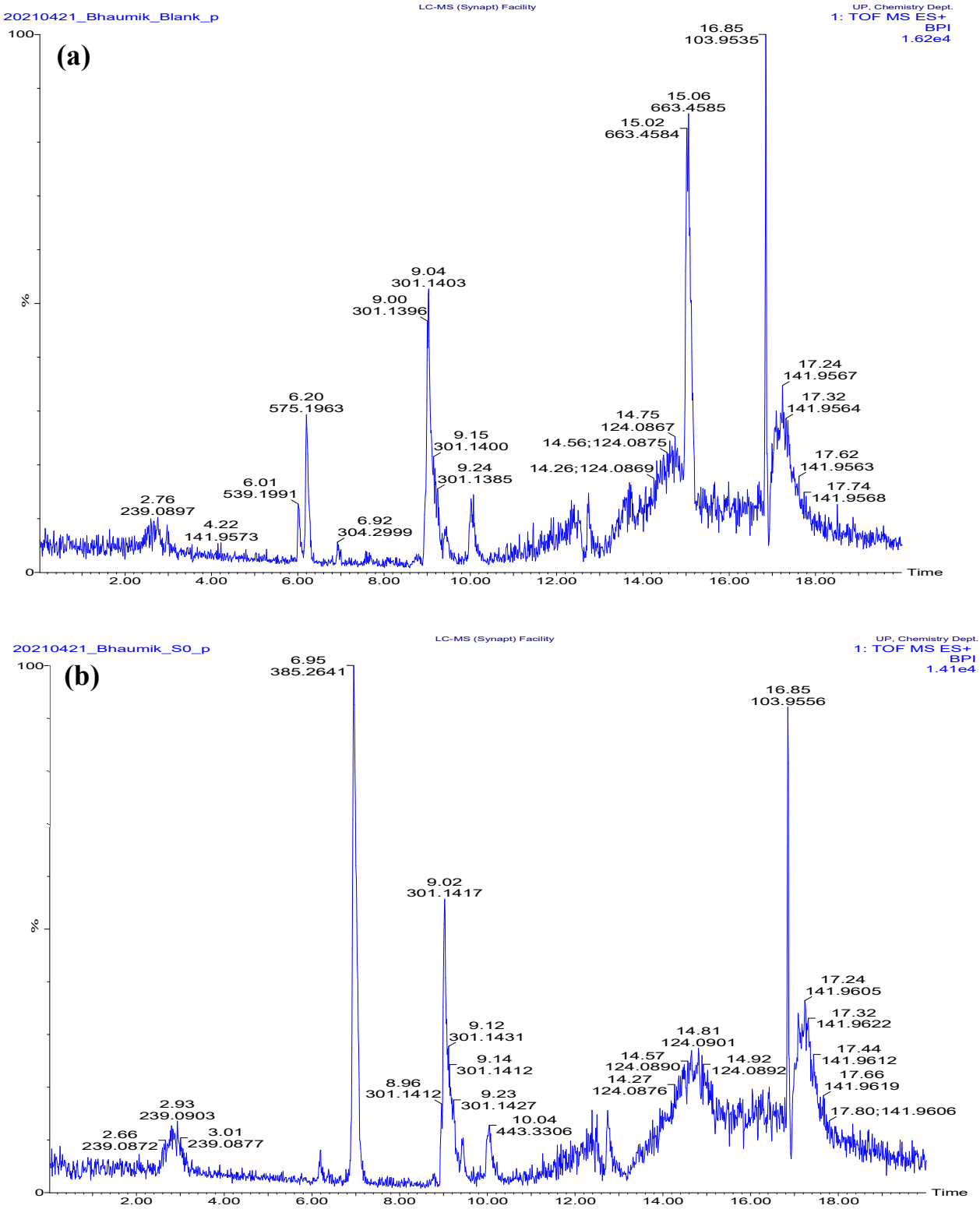

Fig. 10A. LC–MS/MS chromatograms/mass spectra of (a) blank, (b) BG dye before degradation using PANI/Ni^0 NCs + 10 mM H_2O_2 system.

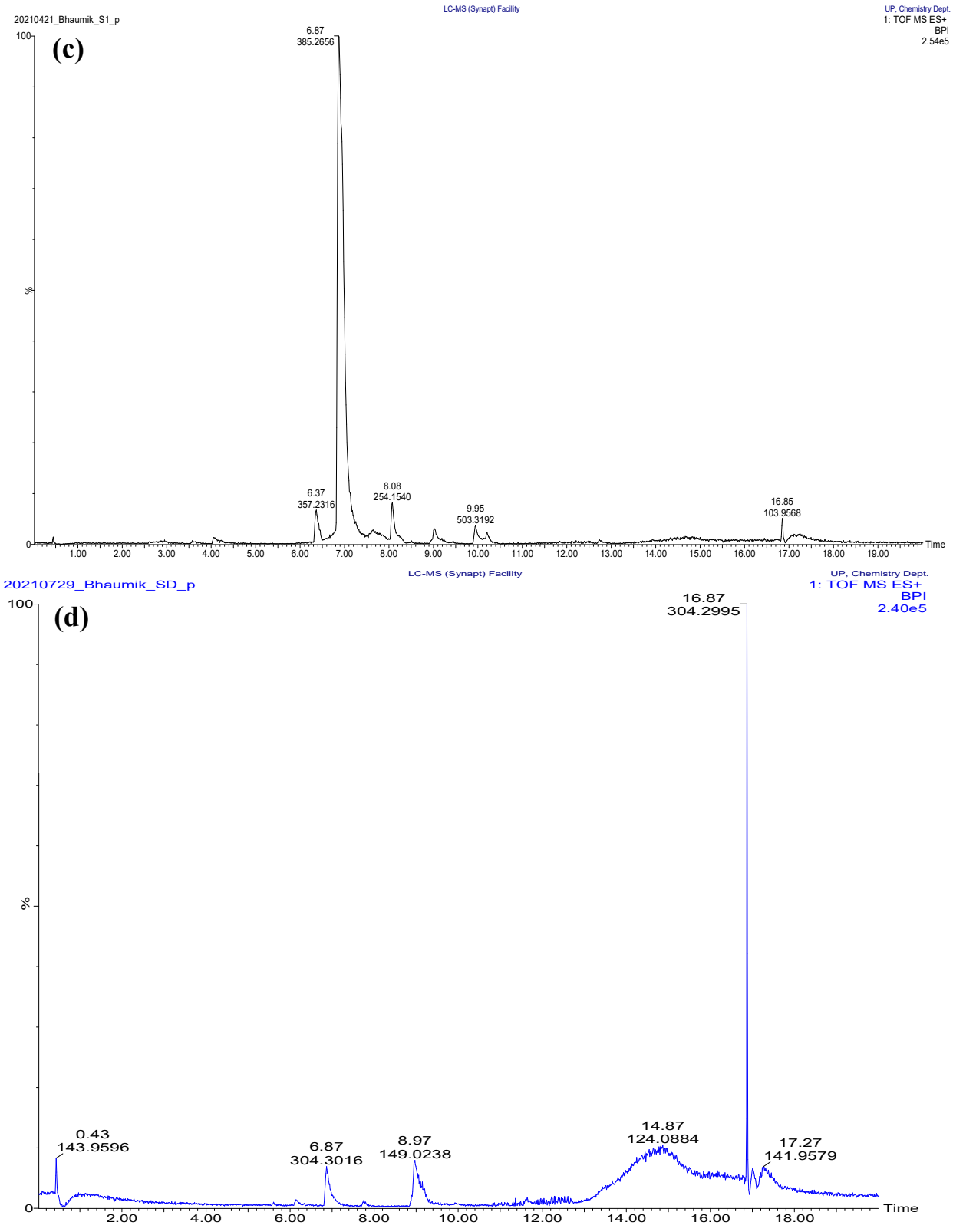

Fig. 10B. LC–MS/MS chromatograms/mass spectra of BG dye degradation (c) after 30 min of degradation reaction and (d) after 120 min of degradation using PANI/Ni^0 NCs + 10 mM H_2O_2 system.

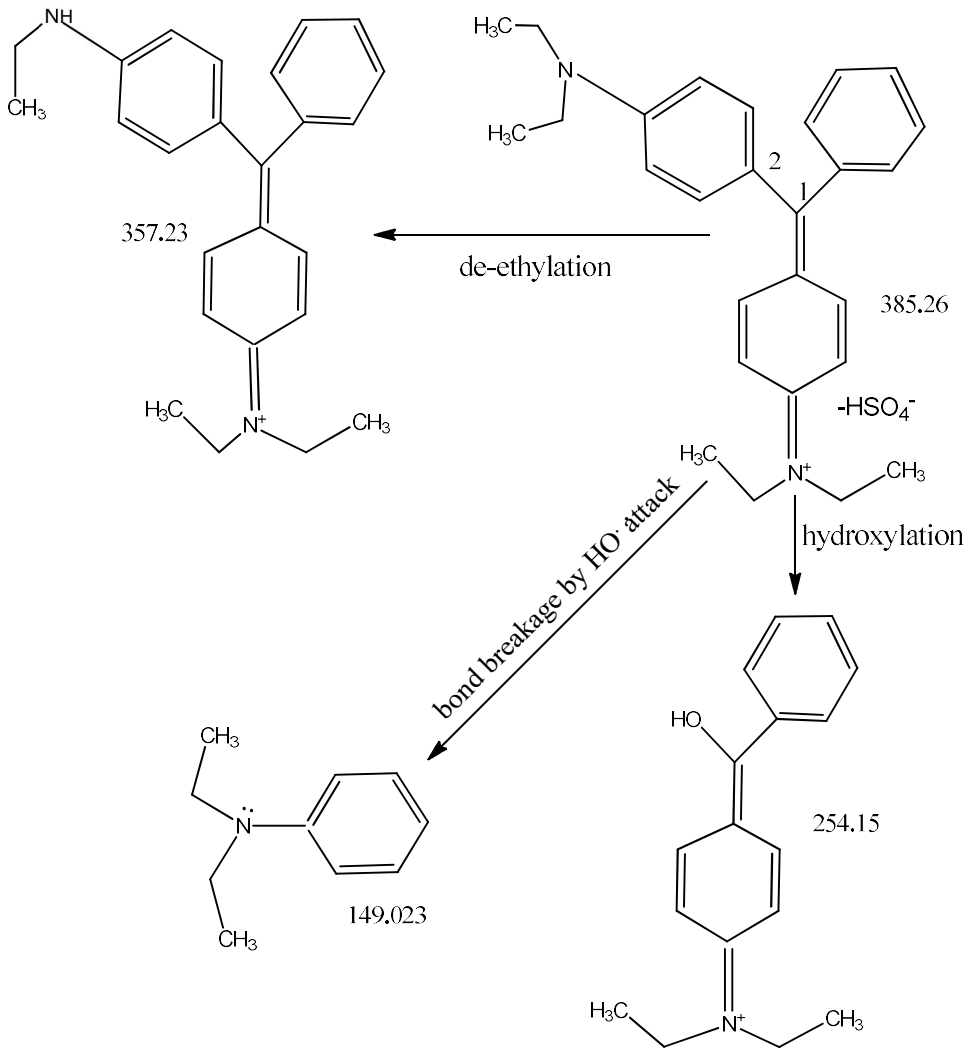

Scheme 1. Plausible pathways of degradation and chemical structure of the major decomposition products of BG before and after treatment with PANI/Ni^0 NCs+10 mM H_2O_2.